



Article

Enhancing Root Distribution, Nitrogen, and Water Use Efficiency in Greenhouse Tomato Crops Using Nanobubbles

Fernando del Moral Torres ^{1,2,*}, Rafael Hernández Maqueda ^{1,3} and David Erik Meca Abad ⁴

¹ Departament of Agronomy, University of Almería, Carretera de Sacramento s/n, La Cañada de San Urbano, 04120 Almería, Spain; rafahm@ual.es

² CIAIMBITAL, Research Centre for Mediterranean Intensive Agrosystems and Agrifood Biotechnology, University of Almería, Carretera de Sacramento s/n, La Cañada de San Urbano, 04120 Almería, Spain

³ Universidad Técnica de Cotopaxi, Av. Simón Rodríguez s/n, Barrio El Ejido Sector San Felipe, Latacunga 050108, Ecuador

⁴ Research Station of Cajamar Las Palmerillas, Cajamar Foundation, Grupo Cooperativo Cajamar, Paraje Las Palmerillas 25, El Ejido, 04710 Almería, Spain; daviderikmeca@fundacioncajamar.com

* Correspondence: fmoral@ual.es; Tel.: +34-950015924

Abstract: The aim of this work was to determine the effect of saturating the irrigation solution with air (MNBA) or oxygen nanobubbles (MNBO) on relevant agronomic, productive, and postharvest parameters of tomato crops (*Solanum lycopersicum* L.) in greenhouses. As a control, conventional management was established, without nanobubbles, under the best possible agronomic conditions used in commercial greenhouses in southeastern Spain. No significant differences were found in the soil properties analysed or in the ionic concentration of the pore water extracted with Rhizon probes. Both MNBA and MNBO modified the root distribution and improved the N uptake efficiency and field water uptake efficiency compared to the control. MNBA had the highest harvest index. The total or marketable production was not affected, although it did increase the overall size of the fruit and the earliness with which they were produced compared to the control. MNBA significantly decreased titratable acidity and soluble solids content compared to the control in the last harvests. Both nanobubble treatments improved postharvest storage under room-temperature (20–25 °C) conditions.



Citation: del Moral Torres, F.; Hernández Maqueda, R.; Meca Abad, D.E. Enhancing Root Distribution, Nitrogen, and Water Use Efficiency in Greenhouse Tomato Crops Using Nanobubbles. *Horticulturae* **2024**, *10*, 463. <https://doi.org/10.3390/horticulturae10050463>

Academic Editor: Rosario Paolo Mauro

Received: 10 April 2024

Revised: 27 April 2024

Accepted: 29 April 2024

Published: 1 May 2024



Copyright: © 2024 by the authors. Licensee MDPI, Basel, Switzerland. This article is an open access article distributed under the terms and conditions of the Creative Commons Attribution (CC BY) license (<https://creativecommons.org/licenses/by/4.0/>).

1. Introduction

Oxygen availability is considered one of the most important factors for plant growth, after water and nutrient availability [1]. Low oxygen and high CO₂ concentrations, such as those that may occur in certain intensive irrigation systems, especially in heavy soils, negatively affect plant growth and productivity [2–4] and may affect the architecture and distribution of the root system [5,6]. In recent decades, many active techniques for soil or substrate aeration have been introduced. Some inject pressurised air into the irrigation water (oxygation [7–12]) or generate macro or micro air bubbles in the irrigation solution [13,14]. Others add oxidising agents to irrigation solutions such as H₂O₂ [15,16], K₂O₂ [17], CaO₂ [18], urea hydrogen peroxide [19,20], or peracetic acid [21]. Most studies indicate that aerated irrigation improves yield and water use efficiency (WUE) by improving the soil root zone environment and increasing crop water and fertiliser absorptions [1,9,22,23]. But others [10,24] argue that the aeration of the solution not only does not have a significant effect on yield but can even delay flowering and fruit set. The techniques used for soil or substrate aeration are costly or have low efficiency [25], and what seems certain is that none of them is being widely used in agriculture as a consequence of either a lack of cost-effectiveness, a lack of experimentation, or a lack of consistent protocols for their application at field scale [7,26,27].

The use of nanobubbles (ultrafine bubbles with a diameter <1 μm , according to ISO 20480-1:2017) in high-frequency irrigation systems is presented as a promising method to improve soil oxygenation, mainly around emitters where hypoxic conditions occur more frequently [8,25,28–30]. Nanobubbles exhibit a large specific surface area, long residence time, high gas–liquid mass transfer efficiency, high zeta potential, and hydroxyl radical production [31–34] and allow for easy implementation in irrigation systems. Additionally, they allow higher levels of dissolved oxygen to be maintained in the aqueous phase compared to traditional aeration methods [35,36].

Our hypothesis is that, even under the best available agronomic conditions of soil and crop management, the introduction of nanobubbles in the irrigation solution in intensive greenhouse growing systems will improve the root distribution of the crop, especially in the areas closest to the emitter where hypoxic conditions are frequent. This will lead to an improvement in nutritional and crop production parameters and postharvest behaviour. The gas composition of the nanobubble will be relevant to this effect.

The aim of this work was to determine the effect of saturating the irrigation solution with air micro-nanobubbles (MNBA) or oxygen micro-nanobubbles (MNBO) on relevant agronomic, productive, and postharvest parameters of tomato crops (*Solanum lycopersicum* L.) in greenhouses. As a control, conventional management was established, without nanobubbles, under the best possible agronomic conditions used in commercial greenhouses in southeastern Spain.

2. Materials and Methods

2.1. Experimental Site

A tomato crop (*Solanum lycopersicum* L) was grown in soil in a plastic greenhouse at the experimental station ‘Las Palmerillas’ (Cajamar Foundation), located in El Ejido, Almería, SE Spain (36° 48' N, 2° 43' W, and 151 m elevation). The greenhouse had a galvanised steel multi-span structure, with 4.5 m to the ridge and a gable roof with an inclination of 30°, covered with a trilaminated low-density polyethylene (LPDE) film (0.2 mm thick). It had no heating and had passive ventilation by means of lateral side panels and flap roof windows whose opening and closing were automatically managed with the climate controller (PrivaWeatherStation. Priva. LC De Lier. The Netherlands).

The soil was an artificial layered ‘enarenado’ typical of greenhouses in the region [37] composed by, from top to bottom, a coarse sand layer acting as an inorganic mulch (0–10 cm depth), a loam soil layer imported from a quarry (10–40 cm depth), and a sandy clay loam original soil (>40 cm depth) of low agronomic quality due to their high stoniness. Before the start of the experiments, the imported soil was ploughed to a depth of 30 cm, with two cross passes using a rigid five double coil tines chisel powered by a Pasquali Siena K5.60 tractor. With ploughing, 3.6 kg m^{-2} of sheep manure (63% dry matter, 1.7% total N content (over dry matter), and 0.7 Mg m^{-3} bulk density), 0.15 kg m^{-2} of agricultural gypsum ($\text{CaSO}_4 \cdot 2\text{H}_2\text{O}$; 23.3% Ca; 18.6% S), 0.4 kg m^{-2} of wheat straw, and 0.037 kg m^{-2} of ammonium nitrate (33.5% N) were incorporated into the soil.

Above-ground drip irrigation was used for combined irrigation and fertigation. Table 1 shows the total volume of water (TVW) used during the crop cycle and the total amount of nutrients supplied in fertigation per treatment. Supplementary Materials Table S1 shows the composition of the fertigation solutions throughout the crop. Drip tape was arranged in single lines with 2.0 m spacing between lines, and 0.25 m spacing between drip emitters within drip lines, given an emitter density of 2 emitters m^{-2} . The emitters had a discharge rate of 1.1 L h^{-1} . The irrigation doses and frequencies were calculated with the PrHo program [38,39] considering the soil moisture content (Supplementary Materials Figure S1), the phenological stage of the crop, and the internal climatic data of the greenhouse (Supplementary Materials Figure S2), in order to optimise the irrigation volumes provided and maintain a soil water tension between 10–20 kPa.

Table 1. Total volume of water (TVW) used during the crop cycle ($\text{m}^3 \text{ ha}^{-1}$) per treatment and total amount of nutrients supplied in fertigation (kg ha^{-1}).

	Control	MNBA	MNBO
TVW	5194	4825	5065
N-NO ₃	573.4	565.1	583.3
N-NH ₄	25.5	24.1	24.8
K ⁺	640.6	681.3	708.1
Ca ⁺⁺	926.1	865.4	901.3
Mg ⁺⁺	388.9	360.7	378.8
SO ₄ ⁼	395.9	423.7	440.3
HCO ₃ ⁻	126.5	126.6	131.0
Na ⁺	980.7	909.6	955.4
Cl ⁻	2822.7	2618.0	2749.8
Fe	7.0	6.5	6.8
Mn	4.0	3.7	3.9
Zn	1.6	1.4	1.5
B	1.3	1.2	1.3
Cu	0.3	0.3	0.3

2.2. Crop

The indeterminate tomato crop (F1 hybrid ‘Harrison’) was transplanted as 6-week-old seedlings on 15 September 2021 and grown until 1 June of 2022 (259 days from transplant to end), with a density of 0.67 plants per square metre (0.75 m between plants on the same row; 2.0 m between rows). The apical stem was pruned to obtain two productive stems per plant (1.33 stems per square metre). The crop management practices (crop training, pruning, and pest management) followed the established best local practices. Pollination was conducted by introducing bumblebees into the greenhouse.

2.3. Experimental Design

2.3.1. Experimental Treatments

To compare the effect of the addition of nanobubbles of oxygen (MNBO) or air (MNBA) in fertigation solutions optimised for tomato cultivation, against a control treatment (C) consisting of the sole application of the nutrient solution, a randomised complete block design was used. The greenhouse was divided into three blocks, each with three rows and 24 plants per row. Two plants at the north and south ends of each row, as well as two rows at the east and west ends of the greenhouse, were excluded from the trial as border areas along the edges of the greenhouse. In each block, one replicate of each treatment was randomly arranged (Supplementary Materials Figure S3).

2.3.2. Generation of Nanobubbles

Bulk nanobubbles were generated via cavitation using the generator equipment model NB 100.6 from the company Nanobubbles S.L. Two reservoir tanks were used where the fertigation solution was saturated with nanobubbles before being pumped into the greenhouse in each irrigation event by means of independent pumping systems (Figure 1). At the greenhouse inlet, a flow meter continuously and independently recorded the incoming volumes for each treatment. Table 2 shows the results obtained from the analysis of five samples of fertigation solutions saturated with nanobubbles of O₂ or air, carried out by the IESMAT company by means of Nanoparticle Tracking Analysis (NTA) (Nanosight NS300. Malvern, UK), the most commonly used method for determining the size and concentration of nanobubbles in water [32,40,41].

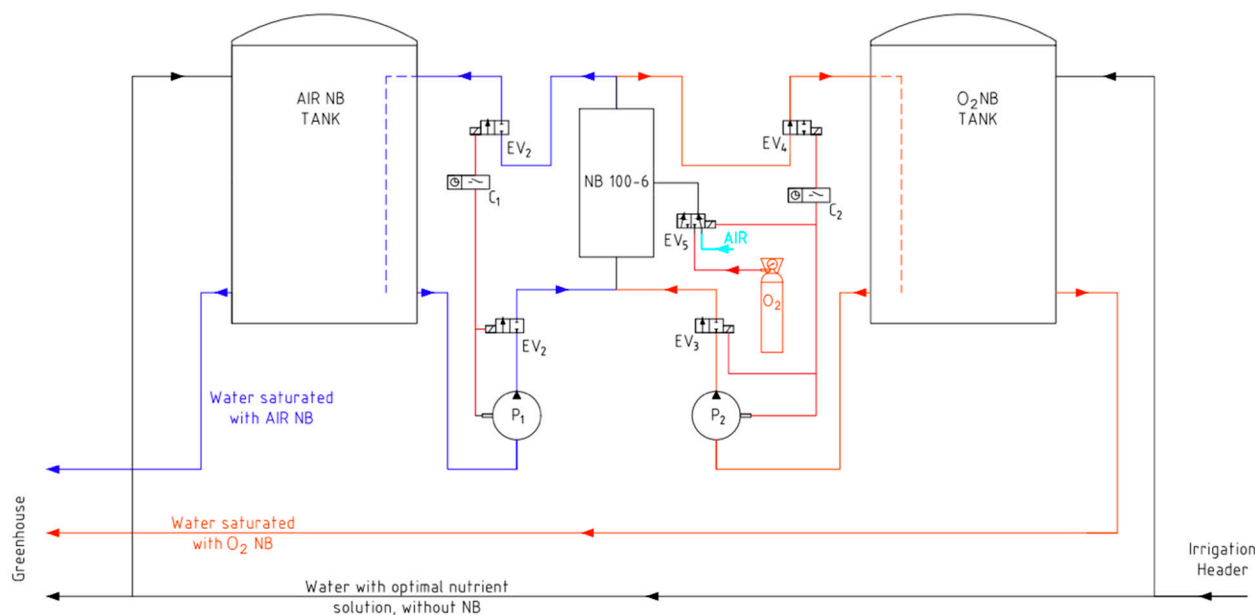


Figure 1. Schematic layout of the nanobubble generation system and distribution of fertigation solutions for the different treatments. EV: solenoid valve; P: pump; NB: nanobubble.

Table 2. Concentration and descriptive parameters of the size distribution of O₂ (MNBO) and air (MNBA) nanobubbles in fertigation solutions used in the experiments. Data show the means \pm standard error (MSE). D10, D50, and D90 percentile values indicate the size below which 10%, 50%, or 90% of all particles are found.

	MNBO	MNBA
Mean (nm)	161.7 \pm 4.5	174.1 \pm 32.9
Mode (nm)	96.1 \pm 2.8	125.2 \pm 32.2
D10 (nm)	89.7 \pm 2.9	110.6 \pm 30.1
D50 (nm)	134.6 \pm 3.8	144.3 \pm 34.1
D90 (nm)	290.9 \pm 8.4	268.8 \pm 27.8
Concentration (particles mL ⁻¹)	2.5 \times 10 ⁸ \pm 1.7 \times 10 ⁷	1.93 \times 10 ⁸ \pm 4.09 \times 10 ⁷

To ensure the correct functioning of the system throughout the trial, the oxygen saturation in the fertigation solutions, in the reservoir tanks, and at the outlet of the drippers was periodically measured with Oxyguard's Handy Polaris 2 TGP portable gas pressure gauge.

2.4. Soil Measurements

2.4.1. Soil Sampling

Soil sampling was carried out twice: (T1) before starting irrigation and transplanting and (T2) immediately before removing the crop. From each replication, three drippers were randomly selected, in each of which three soil subsamples were taken with an auger of 4.5 cm internal diameter at 0–30 cm depths in a triangular arrangement at a distance of 10 cm with a centre in the dripper. All subsamples were mixed in a composite sample per replication. The sand mulch layer was removed before sampling. Once collected, the samples were kept field-moist in polyethylene bags sealed at 4 °C until required.

2.4.2. Soil Analyses

Field-moist samples were air-dried, ground, and sieved to 2 mm. Total organic carbon (TOC) was determined in finely ground soil via wet oxidation [42]. Electrical conductivity (EC, dSm⁻¹) was measured in a 1:5 (*w/w*) soil/water suspension (UNE 77308:2001), with a Crison 522 conductivity meter. pH was measured in a 1:5 (*w/w*)

soil/water suspension (UNE-ISO 10390:2012) with a Crison basic 20-pH meter. Total nitrogen (TN) was measured with an elemental analyser (Elementar Rapid N, Elementar Analysensysteme GmbH. Hanau, Germany). Mineral nitrogen and fractions (Nmin, N-NO₃, and N-NH₄) were determined accordingly Mulvaney [43] after extraction with KCl 2M. Available potassium was determined via flame photometry after extraction with ammonium acetate 1N. Available phosphorus was determined according to the Olsen standard operating procedure proposed by GLOSOLAN [44], after extraction with a dilute solution of NaHCO₃ at pH 8.5.

2.4.3. Soil Pore Water Sampling

Rhizon MOM samplers (10 cm long, 2.5 mm diameter. Rhizosphere research products Wageningen, the Netherlands) were installed 8 cm from the plant, in the zone of influence of the emitter at a depth of 10 cm measured from the surface of the imported soil. Samples of pore water were collected every 15 days by applying vacuum with a syringe set from the same manufacturer. No irrigation was made during the 24 h period of sample collection.

2.5. Crop Measurements

2.5.1. Root Sampling

The root length density was determined by taking three soil cores in each of the treatment replicates. Root sampling was carried out using a hand auger with an internal diameter of 4.5 cm. The full thickness of the imported soil layer, after the removal of the sand layer, was sampled at two depth intervals (0–15 cm and 15–30 cm). Two sampling positions were established in relation to representative plants and emitters: 10 cm perpendicular to the plant, close to the emitter (P1) and 30 cm perpendicular to the plant (P2). Both positions were established in the direction of the passage between crop rows.

The roots of each sample were gently washed to remove any soil particles and were stained with a neutral red solution to obtain more contrast for subsequent scanning. Roots were scanned (Epson Perfection V800. Seiko Epson Corporation. Nagano, Japan) at 400 dpi in greyscale. The WinRhizo Reg 2021 software (Regents Instruments Inc. Quebec, Canada) was used to determine the total root length [39].

The root length density (cm cm^{-3}) was computed using the volume of soil sampled in each layer. The relative root length distribution per soil layer was calculated as the root length of a given soil layer divided by the root length of all layers.

2.5.2. Petiole Sap Nutrient Status

The nutrient content in petiole sap was determined every two weeks. The most recently fully expanded leaves of eight randomly selected plants in each replication were collected and refrigerated before processing in the laboratory within 6 h of sampling [45]. The petiole and fresh leaf blade were separated. Subsequently, the petioles were cut into 1 cm long pieces and then pressed to obtain the sap for analysis. The $[\text{N-NO}_3^-]$ and $[\text{K}^+]$ were determined by means of selective electrodes LAQUAtwin (Horiba Instruments Incorporated. Irvine, CA, USA) without dilution [46].

2.5.3. Above-Ground Dry Matter (Leaves and Stems) Production

All fresh material from the pruning and leaf removal of eight plants in each of the replications was weighted and the dry matter content was determined by oven-drying the representative subsamples at 65 °C to constant weight. At the end of cultivation, all eight plants were removed and their fresh and dry weights, excluding residual fruit, were determined.

2.5.4. Fruit Production and Quality

Replicate areas of 3.2 m², one per treatment within the single block, each with four plants (eight stems), were used to determine the fruit production. There were 23 fruit harvests during cultivation. For each fruit harvest, the fruit fresh and dry weight per plant

were determined. Fresh production was separated into marketable and non-marketable, indicating the reason why the fruit is not marketable (Supplementary Materials Figure S4), according to the Commission-delegated regulation (EU) 2019/428 of 12 July 2018. The separation into classes and sizes was also carried out in accordance with the standard.

On two occasions, external and internal quality checks were carried out on the fruit. (17 February 2022 and 5 April 2022, harvest numbers 11 and 16). In each of the two harvests, for each replicate of each treatment, 10 fruits that had reached physiological maturity were selected. For each fruit, height, diameter, (digital calibre 0–150 mm Inox Novatools) and fresh and dry weights were measured. The fruit colour was determined via direct reading using a chroma-meter CR-400 (Konica Minolta Sensing Americas) expressed using the CIE L*a*b* system. The measurements were taken at three different parts of a fruit and averaged. The colour index (CI) [47,48] was determined according to the following expression:

$$CI = \frac{(1000 \times a^*)}{(L^* \times b^*)} \quad (1)$$

The total colour change (ΔE) [49,50] was calculated using the following expression:

$$\Delta E_{ab}^* = \sqrt{(L_{MNB}^* - L_C^*)^2 + (a_{MNB}^* - a_C^*)^2 + (b_{MNB}^* - b_C^*)^2} \quad (2)$$

where sub-index MNB represents the value for each nanobubble treatment and C represents the values of the control treatment.

A Turoni BC-TR 53,215 hardness tester was used to determine the hardness of the tomato skin. The hardness tester tip selected for the measurements was 0.25 cm². Two measurements were taken in the equatorial zone of each tomato. The fruit firmness was measured in three positions using an Agrosta penetrometer (Penefel DFT 14), with a 0.5 cm² tip surface on a fixed support. To evaluate the internal quality of the fruits, 10 fruits of each replicate of each treatment were collected at random at physiological maturity, and a homogeneous sample of tomato juice was obtained, on which the soluble solids content (SSC, expressed in °Brix), was determined by means of digital refractometer Atago PAL-1. The pH was measured by means of a pH meter HORIBA pH 1500, and titratable acidity (expressed as the percentage of citric acid), was determined titrimetrically using a 0.1 N NaOH solution in the presence of phenolphthalein.

The fruit maturity index [51] was calculated according to the following equation:

$$MI = \frac{SSC(\text{°Brix})}{\text{Titratable acidity}(\% \text{citric acid})} \quad (3)$$

2.5.5. Weight Lost during Postharvest Storage

Ten fruits of each replicate of each treatment were randomly allocated at two storage temperatures: 9 °C and 90% relative humidity (cooling chamber) and room temperature (20–25 °C). The fruits were stored in a ventilated, dark and tempered room for 36 days and their weight loss was assessed every 6 days. The weight lost during postharvest storage was determined by subtracting sample weights from their previous recorded weights and presented as % of weight loss compared to initial weight [52].

2.5.6. Indices

Harvest index (HI) is defined as the ratio between yield (Y) and total biomass produced (yield and leaf and stem biomass, TB) [53]. Field water use efficiency (fWUE) is defined as the yield produced per unit of water used (WU irrigation + fertigation) [54]. Agronomic nitrogen use efficiency (ANUE) is defined as the yield produced per unit of nitrogen applied (AN soil preparation + fertigation) [55]. Agronomic potassium use efficiency (AKUE) is defined similarly.

2.6. Statistical Analysis

Significant differences in tomato agronomic parameters and soil chemical properties across nanobubble treatments were determined using a two-way analysis of variance (randomised block design with block and nanobubble treatments as independent variables with no interaction) and a Tukey test at the significance level of $p < 0.05$ for nanobubble treatments. For those variables that allow comparisons over time, according to the experimental design, an analysis of variance of repeated measures (RM-ANOVA) was used, followed by post hoc least-square difference tests. For the analysis of root length density between the three treatments, factorial ANOVA was used, with four factors: block, nanobubble treatment, soil layer, and sampling position. SPSS software v.29 (SPSS Inc.) was used for statistical processing. The tables and figures were edited with MS-EXCEL (Microsoft Corp.).

3. Results

Table 3 shows the average dissolved oxygen values found for each of the treatments in the tank (MNBA and MNBO nanobubble-saturated treatments) or in the irrigation water storage pond (control) before irrigation and those measured in soil irrigation solutions.

Table 3. Dissolved oxygen concentration (mg L^{-1}) for each treatment. Data show means \pm MSE ($n = 7$).

	Control	MNBA	MNBO
Tank or pond (before irrigation)	5.6 ± 0.7	7.6 ± 0.3	29.78 ± 1.17
Irrigation solution	4.51 ± 0.6	7.0 ± 0.2	24.2 ± 1.7

The concentration of dissolved oxygen in the different treatments was in line with the values reported in other studies using air or oxygen nanobubbles for water aeration [56,57]. The dissolved oxygen values when gaseous oxygen was used as internal gas in nanobubbles were approximately 4 times higher than those achieved when the tank solution was saturated with air nanobubbles and 5.5 times higher than those of irrigation water used as a control.

3.1. Soil Measurements

3.1.1. Soil

The values of the measured edaphic properties, except pH, total nitrogen, and bioavailable potassium, decreased significantly ($p < 0.001$) for all treatments from the initial (T1) to the final values (T2). No significant differential effect was observed between the different treatments applied (Table 4) at the end of the crop.

Table 4. Soil properties at (T1) before starting irrigation and transplanting, and (T2) immediately before the removal of the crop. Data show means \pm MSE ($n = 3$).

	Sampling Time T1	Sampling Time T2		
		Control	MNBA	MNBO
TOC (g kg^{-1})	$10.49 \pm 2.77^{\text{a}}$	$6.7 \pm 1.3^{\text{b}}$	$6.3 \pm 1.2^{\text{b}}$	$4.4 \pm 1.8^{\text{b}}$
pH	8.53 ± 0.31	8.57 ± 0.21	8.53 ± 0.15	8.53 ± 0.12
EC (dS m^{-1})	$0.77 \pm 0.4^{\text{a}}$	$0.53 \pm 0.09^{\text{b}}$	$0.60 \pm 0.02^{\text{b}}$	$0.52 \pm 0.0^{\text{b}}$
P (g kg^{-1})	$0.21 \pm 0.11^{\text{a}}$	$0.16 \pm 0.01^{\text{b}}$	$0.14 \pm 0.04^{\text{b}}$	$0.15 \pm 0.03^{\text{b}}$
K (g kg^{-1})	2.40 ± 0.69	2.33 ± 0.58	2.83 ± 0.58	2.17 ± 0.29
Ntot (g kg^{-1})	1.19 ± 0.29	1.08 ± 0.15	0.93 ± 0.11	1.00 ± 0.26
Nmin (mg kg^{-1})	$25.62 \pm 17.7^{\text{a}}$	$14.62 \pm 5.79^{\text{b}}$	$15.45 \pm 6.86^{\text{b}}$	$13.89 \pm 4.46^{\text{b}}$
N-NO ₃ (mg kg^{-1})	$17.48 \pm 15.84^{\text{a}}$	$8.37 \pm 7.67^{\text{b}}$	$8.51 \pm 5.04^{\text{b}}$	$7.64 \pm 2.21^{\text{b}}$
N-NH ₄ (mg kg^{-1})	$8.14 \pm 5.69^{\text{a}}$	$6.25 \pm 3.67^{\text{b}}$	$6.94 \pm 2.18^{\text{b}}$	$6.25 \pm 3.7^{\text{b}}$
NO _{3s} ⁻ (mg L^{-1})	$351 \pm 134^{\text{a}}$	$317 \pm 61^{\text{b}}$	$330 \pm 157^{\text{b}}$	$277 \pm 55^{\text{b}}$
K _s ⁺ (mg L^{-1})	$62.5 \pm 41.0^{\text{a}}$	$27.3 \pm 1.5^{\text{b}}$	$24.0 \pm 5.1^{\text{b}}$	$26.3 \pm 5.7^{\text{b}}$

Table 4. Cont.

Sampling Time	Sampling Time T2			
	T1	Control	MNBA	MNBO
Sand (% w/w)	45.3 ± 2.8	-	-	-
Silt (% w/w)	34.3 ± 3.0	-	-	-
Clay (% w/w)	20.4 ± 1.0	-	-	-

Different letters in the same row indicate significant differences ($p < 0.001$) between treatments. TOC: total organic carbon; EC: electrical conductivity; P: available phosphorus; K: available potassium; Ntot: total nitrogen; Nmin: mineral nitrogen; NO₃s: pore water NO₃; K_s: pore water K. Sand, silt, and clay expressed in % w/w according to the USDA's classes.

3.1.2. Soil Pore Water

The N-NO₃ concentration in soil pore water evolved in a similar way in all treatments, with no statistically significant differences between them (Figure 2, left column). Values were high at the beginning of the crop, during vegetative development, and tended to decrease over time in a similar way in all treatments. The potassium concentration in soil pore water (Figure 2, right column) showed no significant differences between treatments. In all cases, the potassium concentration tended to increase towards the end of the crop.

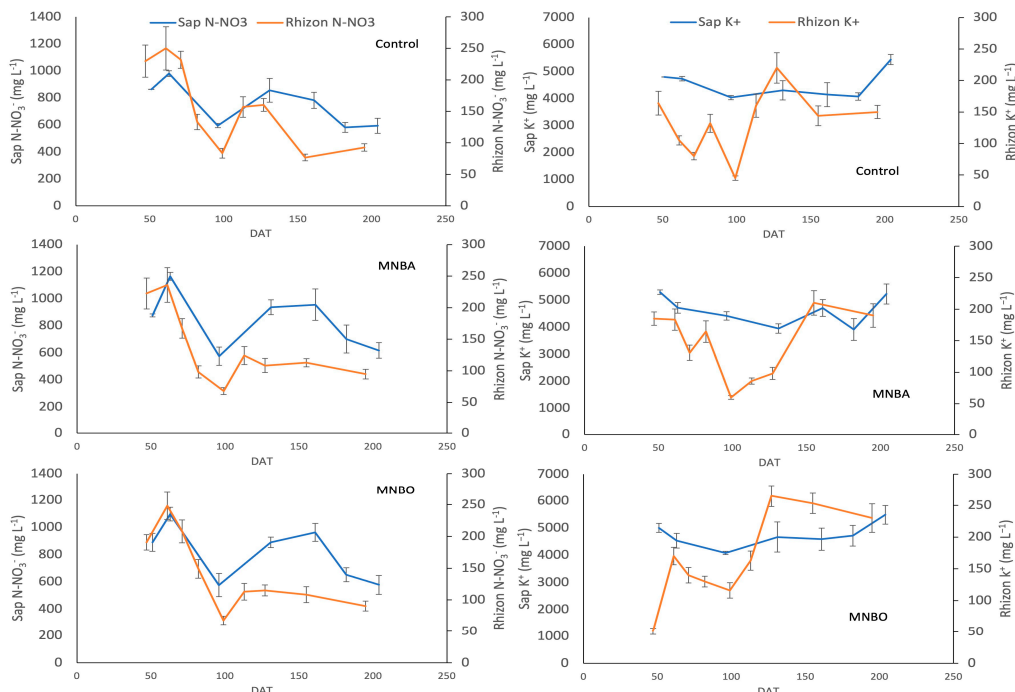


Figure 2. Left column: evolution over time of pore water N-NO₃⁻ obtained via Rhizone MOM samplers and sap N-NO₃⁻ concentrations in each treatment. Right column: evolution over time of K⁺ concentrations. Data show means ± MSE. DAT stands for the date after transplanting.

3.2. Crop Measurements

3.2.1. Root Length Density

The root length density decreased from the plant's main stem outwards in the three treatments (Figure 3). The total root length density, considering all sampling positions and depths, was significantly lower for the control treatment ($0.22 \text{ m}^3 \text{ m}^{-3} \pm 0.02 \text{ MSE}$) than for the MNBA ($0.73 \text{ m}^3 \text{ m}^{-3} \pm 0.08 \text{ MSE}$) and MNBO ($0.89 \text{ m}^3 \text{ m}^{-3} \pm 0.08 \text{ MSE}$) treatments.

The root length density was significantly higher in nanobubble treatments in all sample positions except in the surface layer of the sampling position P2, the furthest from the plant stem, for which we did not find significant differences.

At position P1, the differences between both nanobubble treatments and the control were at their maximum in the entire profile. At this position, in the deepest layer, the nanobubble treatments differed from each other, with the highest root length density for the MNBO treatment. The MNBA treatment showed intermediate values of root length density between the control and MNBO at this position.

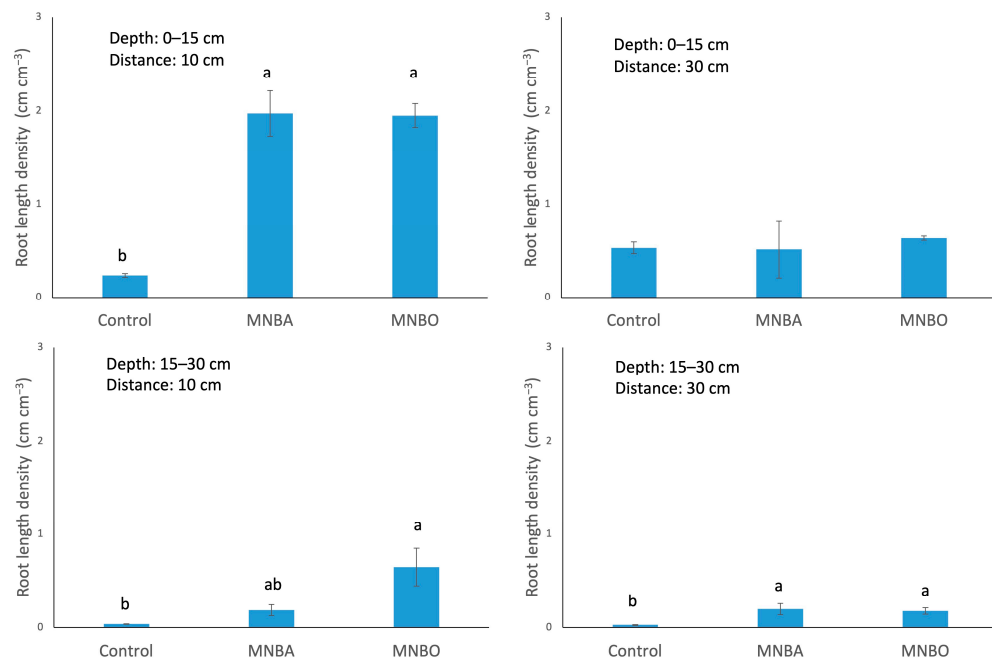


Figure 3. Root length density per soil layer sampled in the two sampling positions (P1, 10 cm from the plant; P2 30 cm from the plant). C, control; MNBA: micro-nanobubbles of air; MNBO micro-nanobubbles of oxygen. Different lowercase letters in each graph show significant differences among treatments ($p < 0.05$). Data show means \pm MSE.

At sampling position P2, in the deepest layer, the nanobubble treatments showed significantly higher root length density than the control but did not differ from each other.

Relative root length distribution showed a shallower distribution of the root system for the control treatment (Figure 4, left): 92.1% of the root length density was in the upper 15 cm, compared to only 75.8% in the MNBO treatment. However, it was distributed further away from the main stem: 67.2% of its root length density was at the sampling position P2, compared to 24% in the nanobubble treatments. (Figure 4, right).

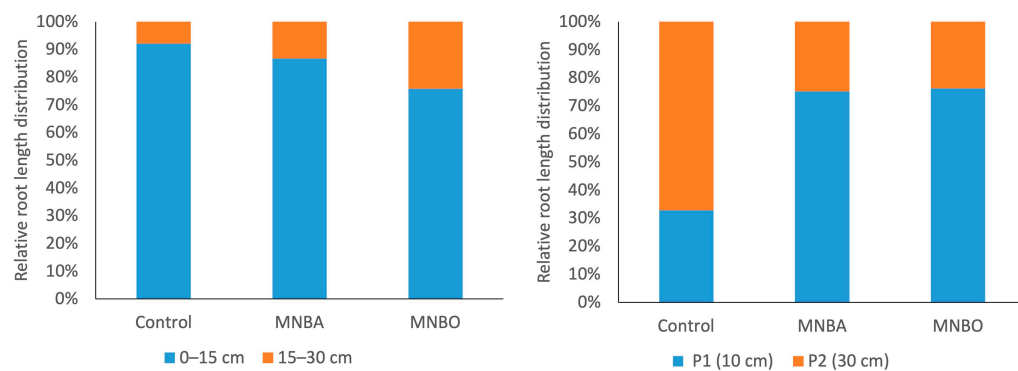


Figure 4. **Left:** relative root length distribution by soil layer depth. **Right:** relative root length distribution by sampling position.

The average root diameter was larger for the control treatment (0.394 ± 0.127 mm) than for the MNBA (0.352 ± 0.063 mm) and MNBO (0.385 ± 0.067 mm) treatments, although there were no statistically significant differences between them.

3.2.2. Petiole Sap

The concentration of N-NO₃ in sap decreased significantly ($p < 0.001$) as the growing season progressed, for all treatments, and presented a similar evolution, desynchronised in time, with the values of N-NO₃ found in the pore water obtained using Rhizon probes. (Figure 2). The average concentration of N-NO₃ in sap in the control (720 ± 76) was significantly lower ($p < 0.05$) than that obtained for the MNBA (819 ± 23) and MNBO (830 ± 40) treatments. No differences were observed for the N-NO₃ concentration in sap as a function of the gas used in the nanobubbles.

The evolution of the potassium concentration in sap (Figure 2) was similar for all treatments, with no significant differences between treatments throughout the season.

3.2.3. Above-Ground Fresh and Dry Matter (Leaves and Stems) Production

The production of above-ground (leaves and stems) fresh and dry matter was higher in the MNBO treatment. (Figure 5, left), with the lowest values found for the MNBA treatment. The differences in accumulated production were noticeable from the first sampling, although it was from the middle of the season (150 DAT) that they became more evident (Figure 5, right).

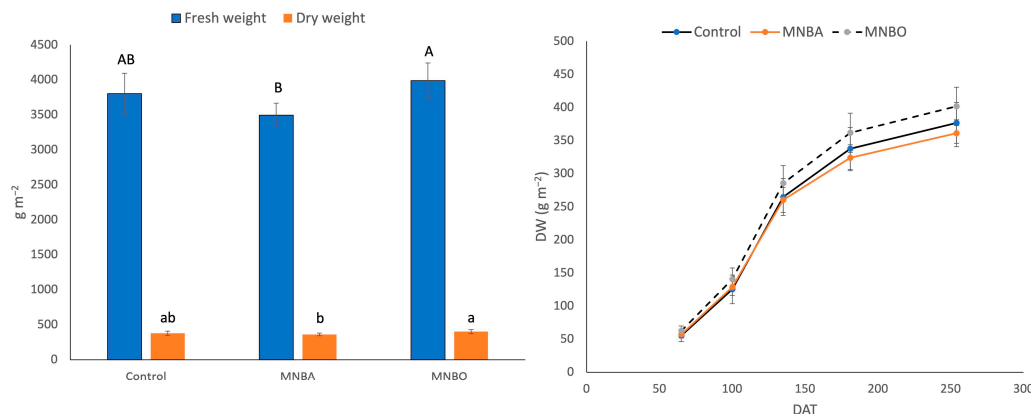


Figure 5. Left: mean above-ground (leaves and stems) fresh and dry matter weights for each treatment. Different capital letters indicate differences ($p < 0.05$) in fresh weight between treatments. Different lowercase letters indicate significant differences in dry weight between treatments. **Right:** evolution of cumulative above-ground (leaves and stems) dry weight over the growing season for each treatment. DAT stands for the date after transplanting. Data show means \pm MSE.

3.2.4. Fruit Production and Quality

There were no significant differences between treatments for either total or marketable production (Table 5), although the nanobubble treatments obtained higher average values than the control in both cases. However, the MNBO treatment showed lower values of non-marketable fruits ($p < 0.1$) compared to the control treatment. The main cause of fruit rejection was Blossom-End Rot (BER). The percentage of fruit affected by BER with respect to the total rejected fruit was 74.2% in the control treatment, compared to 63.6% for the MNBA treatment and 61.2% for the MNBO treatment (Supplementary Materials Figure S4).

The Class I/Class II ratio was in favour of the control treatment (2.33) compared to MNBA (2.14) and MNBO (2.21).

Although there were no significant differences in total dry matter production, the control treatment produced more total dry matter per unit of fresh weight, as expressed by the fresh-to-dry total weight ratio.

Table 5. Yield parameters expressed in Mg ha^{-1} . Data show means \pm MSE. Data are expressed as fresh weight unless otherwise stated.

	Control	MNBA	MNBO
Total	113.02 ± 2.43	118.79 ± 6.97	117.79 ± 3.8
Marketable	97.2 ± 3.82	103.65 ± 8.73	103.57 ± 5
Non-marketable	15.82 ± 2.01	15.14 ± 1.88	14.21 ± 1.44
Class I	67.14 ± 4.1	68.94 ± 5.63	70.91 ± 3.9
Class II	28.08 ± 3.14	32.18 ± 3.62	31.99 ± 3.2
Total Dry weight	10.57 ± 0.87	10.43 ± 0.50	10.18 ± 0.68
Ratio Fresh/Dry weight	10.69	11.39	11.57

The cumulative production classified by category showed a significant increase in the proportion of G-size fruits (size code 8, $>67 \leq 82$ mm) in the nanobubble treatments compared to the control treatment (Figure 6). The control treatment ceased to produce G-size fruits 139 days after transplanting, while the G-size fruit production in the nanobubble treatments was maintained until 155 days after transplanting. The MNBA treatment showed a higher proportion of MM-size fruit (size code 6, $>47 \leq 57$ mm), while the MNBO treatment showed a higher proportion of MMM-size fruit (size code 5, $>40 \leq 47$ mm). The differentiation in the production of these sizes with respect to the control occurred in the final third of the production period. It was the nanobubble treatments that maintained the highest production levels towards the end of the season.

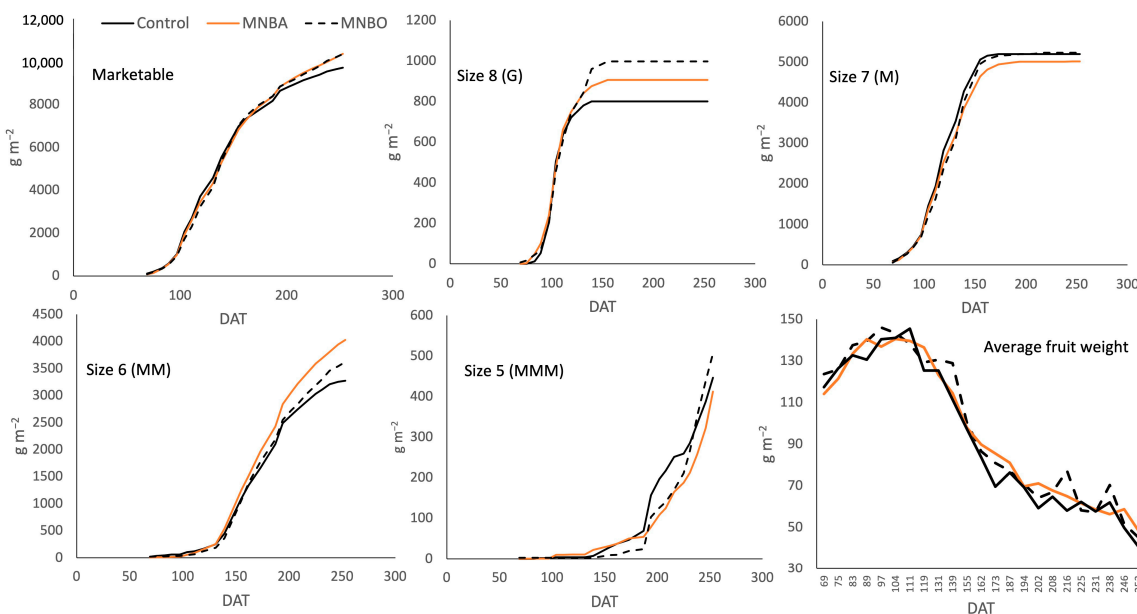


Figure 6. Cumulative commercial production expressed by category for each treatment. Bottom right, average fruit weight at each harvest for each treatment. DAT: days after transplanting.

Table 6 shows the average results of the comparison of different parameters used for the evaluation of the internal and external quality of the fruit carried out for two specific harvests. The fresh fruit weight tended to decrease between the two harvest dates in general for all treatments. The MNBO treatment consistently showed significantly higher fruit weight than the control treatment. The MNBA treatment produces fruit with significantly higher fruit weight in the second harvest. Fruit acidity generally decreased over time, although there were no significant differences in acidity between the different treatments. However, in the later harvest, the fruits from MNBA showed lower titratable acidity than the control. The MNBO treatment occupied an intermediate position.

Table 6. Mean values ($n = 30$; mean \pm MSE) for internal and external quality parameters in tomato fruits. Fresh weight (g); titratable acidity (% citric acid); soluble solid (°Brix); axial diameter (mm); equatorial diameter (mm); hardness (shore); firmness (kg); wall thickness (mm). n.d., no data. Different letters for each treatment in the same row indicate significant differences between treatments ($p < 0.05$) for the same time.

	Time 1: 18/2/2022			Time 2: 5/4/2022		
	Control	MNBA	MNBO	Control	MNBA	MNBO
Fresh weight	116.36 \pm 3.2 ^b	107.5 \pm 2.47 ^b	145.42 \pm 7.91 ^a	67.22 \pm 3.75 ^b	78.84 \pm 4.50 ^a	72.00 \pm 7.10 ^{ab}
pH	3.87 \pm 0.15	3.81 \pm 0.12	3.88 \pm 0.12	4.36 \pm 0.04	4.44 \pm 0.1	4.36 \pm 0.05
Titratable acidity	0.47 \pm 0.04	0.47 \pm 0.02	0.46 \pm 0.02	0.54 \pm 0.03 ^a	0.49 \pm 0.02 ^b	0.53 \pm 0.03 ^{ab}
Soluble solids	5.43 \pm 0.15	5.57 \pm 0.20	5.20 \pm 0.06	6.68 \pm 0.17 ^a	5.48 \pm 0.39 ^b	6.33 \pm 0.44 ^{ab}
Maturity index	11.8 \pm 1.12	11.86 \pm 0.79	11.27 \pm 0.41	12.35 \pm 0.34	11.21 \pm 0.63	11.8 \pm 0.34
Axial diameter	60.35 \pm 1.27	60.04 \pm 0.95	61.71 \pm 1.52	52.44 \pm 1.06 ^b	57.36 \pm 1.89 ^a	53.19 \pm 2.31 ^b
Equatorial diameter	58.48 \pm 0.64 ^b	56.45 \pm 0.84 ^b	63.8 \pm 1.18 ^a	47.95 \pm 1.18 ^b	50.24 \pm 1.31 ^a	47.97 \pm 2.07 ^b
Hardness	67.00 \pm 1.5	70.40 \pm 1.5	72.40 \pm 3.5	85.80 \pm 3.9	88.00 \pm 1.7	89.10 \pm 1.9
Firmness	3.30 \pm 0.08	3.55 \pm 0.1	3.71 \pm 0.27	4.15 \pm 0.09	4.08 \pm 0.11	4.15 \pm 0.11
Wall thickness						
L	37.55 \pm 0.5	37.28 \pm 0.56	37.05 \pm 0.57	37.72 \pm 1.6	38.42 \pm 1.25	36.09 \pm 2.37
a	15.64 \pm 1.09	15.95 \pm 1.36	17.48 \pm 1.04	21.55 \pm 1.16	22.72 \pm 0.22	20.5 \pm 1.25
b	15.28 \pm 0.64	15.86 \pm 0.35	15.69 \pm 0.25	16.65 \pm 0.56	17.03 \pm 0.36	15.48 \pm 1.23
Colour index	27.88 \pm 2.72	27.39 \pm 2.72	30.47 \pm 2.21	34.4 \pm 1.43	34.9 \pm 1.49	37.73 \pm 4.13
ΔE MNBo-Control		1.47 \pm 0.28	3.34 \pm 0.82		4.06 \pm 2.2	2.28 \pm 1.95

The soluble solids content, expressed as °Brix, tended to increase over time, although only in the second harvest did we find significant differences. The MNBA treatment had significantly lower values for this parameter, and the control had the highest. The maturity index did not show significant differences between treatments.

The equatorial diameter of the fruit decreased with time for all treatments. The MNBO treatment showed significantly higher values than the others in the first harvest evaluated, while the MNBA treatment showed the highest values in the second harvest. In this harvest, the fruits from the MNBA treatment also showed significantly greater axial diameters.

Both the hardness and firmness of the fruits tended to increase with time in all treatments but without significant differences between them.

The colour index increased in the second harvest compared to the first one in a general way for all treatments, so that the fruit colours were closer to deep red. The MNBO treatment showed a higher colour index, but not significantly different from the other treatments, in both harvests. However, the results obtained from analysis ΔE showed that the differences in colour between the fruits obtained from the MNBO treatment with respect to the control were perceptible to the human eye at a glance ($\Delta E > 2$) already in the first harvest. In the case of the colour difference between MNBA and the control, estimated according to ΔE , it could only be perceived after careful observation ($1 < \Delta E < 2$). In the second harvest evaluated, both treatments showed colour differences perceptible to the human eye at a glance compared to the control.

3.2.5. Weight Lost during Postharvest Storage

The weight loss of fruit stored at room temperature (20–25 °C) was higher than that of fruit stored in a cooling chamber (Figure 7). The rate of weight loss at room temperature was $0.39\% \pm 0.01$ per day and in the cooling chamber was $0.31\% \pm 0.05$ per day. At room temperature, the nanobubble treatments showed a significantly ($p < 0.01$) lower postharvest storage weight loss than the control (Figure 7), with no differences depending on the type of gas used in the nanobubbles. In cold storage, the weight loss was similar for all treatments, with no significant differences.

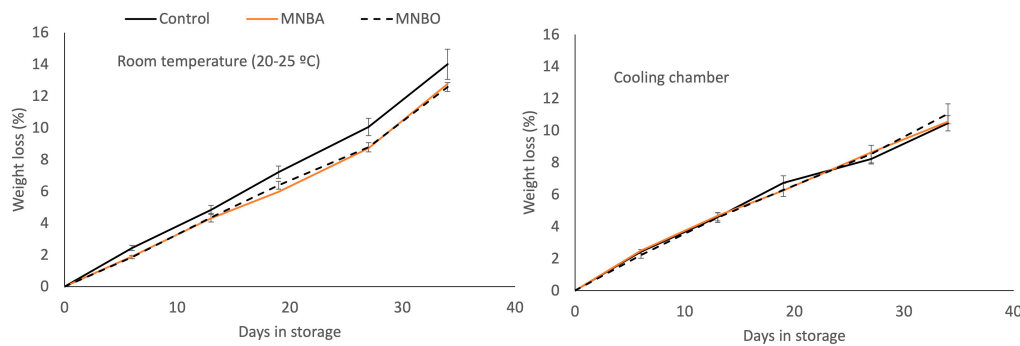


Figure 7. Average percentage ($n = 10$) of postharvest weight loss during conservation at room temperature (left) and in the cooling chamber (right). Data show means \pm MSE.

3.2.6. Indices

The harvest index, field water use efficiency (fWUE), N agronomic use efficiency, and K agronomic use efficiency are shown in Table 7. The MNBA treatment showed the highest values for all calculated indices, followed by the MNBO treatment, with the exception of the harvest index, for which the control treatment showed better values than MNBO.

Table 7. Harvest index, agronomic nitrogen use efficiency (ANUE), agronomic potassium use efficiency and field water use efficiency for each treatment.

	Harvest Index	ANUE	AKUE	fWUE (kg m^{-3})
Control	73.69	123.44	111.37	21.76
MNBA	74.25	131.11	112.54	24.62
MNBO	71.71	127.36	111.83	23.26

4. Discussion

The number of field studies in intensive horticulture that are focused on the effect of the use of nanobubbles through fertigation is still limited, and even more so for those that present data on root distribution or have been carried out in comparison with controls under non-production-limiting conditions, although their number in incubation, column or pot, and substrate conditions is growing.

4.1. Soil Measurements

The use of nanobubbles in the irrigation water has not resulted in significant differential changes in soil properties at the end of the crop, between the different treatments (Table 4), nor in the differential evolution of the N-NO_3^- or K^+ content in the pore water extracted with Rhizon throughout the season (Figure 2), which seems to depend on the ionic concentration of the nutrient solution supplied with the irrigation, common to all treatments (Supplementary Materials Table S1). These results coincide with those obtained by Bonachela et al. [24] in tomato oxyfertigation on rockwool slabs for which the ionic contents of the leached nutrient solution were similar in all treatments. Wu et al. [58], on the contrary, in soil column studies with tomato crops, argue that the use of aerated solutions with nanobubbles significantly increases N release when organic fertilisers are added to the soil. The decrease in the average organic carbon values found in the MNBO treatment, although it does not show statistically significant differences with respect to the control, is higher than that found by authors such as Chen et al. [59] in greenhouse tomato cultivation using nanobubbles.

4.2. Crop Measurements

4.2.1. Root Length Density and Petiole Sap

The nanobubble treatments showed a higher root length density than the control treatment (Figure 3), colonising more densely the areas closer to the emitters and the deeper

horizons. This effect was greater when the gas used was oxygen. Similar results have been obtained by Jin et al. [5] in pumpkins with aerated irrigation, or by Wang et al. [20], who found that oxygenation significantly promoted root development, mainly in the form of longer root length and increased root surface area.

The control treatment distributes its roots proportionally further away from the water emission zone and more superficially than the treatments incorporating nanobubbles. This root distribution in the control management has already been described by Padilla et al. [39] in greenhouse pepper cultivation in the province of Almería and may be due to situations of continued hypoxia as a result of the combined effect of the decrease in air-filled porosity due to the high relative saturation of the soil maintained constantly throughout the crop (Supplementary Materials Figure S1) [60,61] and low dissolved oxygen in irrigation water [62]. Hypoxia conditions, which weaken the aerobic respiration of roots, modify root distribution [6,23,63,64] and can result in decreased energy metabolism and reduced crop yield. The presence of nanobubbles with low buoyancy, high persistence in the irrigation solution, and strong gas mass transfer ability allows air or oxygen to be continuously dissolved in the soil pore water which will favour root respiration in the moisture-saturated zones around the emitter and at depth, increasing the efficiency of water and nutrient uptake [22,63,65]. This effect seems to translate into higher values of the ANUE (agronomic nitrogen use efficiency) and fwUE (field water use efficiency) indices obtained for the nanobubble treatments (Table 7). This increase in nitrogen use efficiency may account for the significantly higher nitrogen concentrations in sap found in treatments incorporating nanobubbles, despite the fact that the ionic contents of pore water in the soil do not differ between treatments throughout the crop.

Petiole sap analysis in conducting tissue is considered to be a sensitive indicator that reflects crop status at the time of sampling [45]. These authors propose a threshold value for optimal crop N nutrition of tomatoes of 1050 mg of $\text{NO}_3\text{-N L}^{-1}$. This threshold value does not include the early establishment and final fruit production phases. According to this threshold, N- NO_3 values in sap have been below the optimum in the final stages of the crop, which, according to these authors, indicates insufficient nitrogen fertilisation, which has been partially mitigated through the application of nanobubbles in the irrigation water.

The reduction in the incidence of Blossom-End Rot (BER) compared to the control for the nanobubble treatments (Supplementary Materials Figure S4), especially in the MNBO treatment, may also be related to the greater efficiency in water use and access to the wettest areas of the soil where water is available at lower tension at times when evapotranspirative demand is higher [66]. In this sense, Wang et al. [67] indicate that changes in root system architecture as a consequence of high oxygen concentrations in irrigation solutions treated with nanobubbles reduce the environmental stress suffered by the roots, thereby improving their ability to obtain nutrients over longer distances. This aspect could be determinant in a differential calcium absorption that would mitigate the appearance of BER. Another hypothesis that could contribute to explain a lower tendency to suffer BER when using oxygen nanobubbles in irrigation is derived from studies carried out by Baram et al. [25], in which they found a significant reduction in the membrane leakage and osmotic potential of lettuce leaf cells when the concentration of dissolved oxygen is increased in irrigation solutions as a result of the incorporation of oxygen nanobubbles. Further studies seem necessary to confirm these results.

4.2.2. Above-Ground Fresh and Dry Matter (Leaves and Stems) Production

The production of above-ground leaf and stem fresh and dry weight is higher in the MNBO treatment (Figure 5). Similar results have been obtained in tomato pot culture by Niu et al. [64]; by Wu et al. [58] in soil column culture, who also find greater differentiation in the early stages of the crop; and by Liu et al. [57] in soil culture in greenhouses. However, Bonachela et al. [24] found no significant differences in biomass production in rockwool cultivation. The MNBA treatment shows significantly lower biomass production than the MNBO treatment, although its harvest index is the highest of all treatments.

4.2.3. Fruit Production, Quality, and Weight Lost during Postharvest Storage

In contrast to most of the reviewed studies, which indicate that irrigation with nanobubbles increases tomato yields [22,25,57,58,68], we found no significant differences in total or marketable production, although the average values of marketable production obtained with the nanobubble treatments are 6.6% higher than those obtained with the control (Table 5). However, the nanobubble treatments result in changes in crop quality parameters: size 8 production is higher for the nanobubble treatments, especially for the MNBO treatment, is earlier than the control, and lasts for a longer period of time (Figure 6). Towards the end of the crop, fruit sizes decrease in all treatments, although the MNBA treatment produces significantly larger fruit sizes than the control. However, it is the control treatment that has the lowest fresh/dry weight ratio. There is a traditional controversy as to whether the regulation of dry matter accumulation in fruit is sink- or source-dependent [69], but some authors argue that lower nitrogen contents, such as those found in the control treatment in the sap analysis, can enhance the sink strength of the fruit, leading to the increased accumulation of dry matter [70]. This, together with the smaller size reached by the fruits of the control treatment, could explain the lower fresh/dry weight ratio found in the control treatment.

In the last harvests, the MNBA treatment shows the lowest titratable acidity and soluble solids values and the highest fruit wall thicknesses, only slightly higher than those found for MNBO (Table 6). This characteristic may contribute to explaining the better postharvest preservation performance under room temperature of the fruit treated with nanobubbles (Figure 7). Pavan et al. [71] find a positive correlation between fruit self-life and pericarp thickness, mediated via yield/plant, titratable acidity, fruit firmness, and soluble solids. Cvirkic et al. [72] also indicate that the increased thickness of the pericarp allows the shelf life and postharvest preservation of tomato fruits to be extended.

The colour of the fruit is also affected by the nanobubble treatments, especially in the last harvests. The differences in colour, towards a deeper red, are accentuated between the nanobubble treatments and the control, being more intense in the MNBO treatment, which may influence the commercial value of the fruit [73]. Several authors have found a significant increase in redness in tomato fruits due to oxygation [74,75] but the final mechanism by which the increase of dissolved oxygen in the irrigation solution modifies fruit colour has not been satisfactorily explained. The effect of water and mineral nutrient use efficiency on fruit colour has been studied, but the results obtained are contradictory [76]. Only recently, Yao et al., [77] using hydrogen-rich water irrigation, provide a plausible explanation indicating that the increase in fruit redness may be linked to an enhanced activation of carotenoid-producing genes, especially lycopene.

4.3. Recommendations and Limitations

This study was carried out over one season on a long-cycle tomato crop (256 days duration and 148 irrigation events). The experimental design is valid to draw conclusions, but some of the soil quality indicators evaluated may have a different response in the long term if the oxidising conditions are maintained over time. Therefore, it will be interesting to study the effect of continuous irrigation with nanobubbles on the properties that define soil quality in a long-term field study.

5. Conclusions

This study demonstrated that the introduction of nanobubbles in the irrigation solution modifies the root distribution of tomato roots grown in soil in Mediterranean greenhouses, especially in areas close to the dripper and in the deepest horizons. It also improves the harvest index, the agronomic N uptake efficiency, and the field water uptake efficiency. In this sense, air as the internal gas of the nanobubble is more efficient than oxygen. However, this effect does not translate into a significant increase in total harvest, although it does increase the overall size of the fruit and the earliness with which they are produced compared to

the control. The use of nanobubbles modifies quality parameters relevant to the commercialisation of the fruit and improves postharvest storage at room-temperature conditions.

Supplementary Materials: The following supporting information can be downloaded at <https://www.mdpi.com/article/10.3390/horticulturae10050463/s1>: Table S1. Ion concentration of irrigation water and irrigation solutions (mmol/L). DAT: Days after transplanting. Expresses time interval with the same concentration; Figure S1. Evolution of the relative saturation (Q) of the soil at 5 cm from the emitter, towards the corridor, and 15 cm deep. DAT: Days after transplanting. Data are expressed as percentages of saturation. Error bars indicate \pm MSE; Figure S2. Evolution of mean temperature ($^{\circ}$ C. top) and mean relative humidity (%. bottom) both inside and outside the greenhouse over the time period of the trials. DAT: Days after transplanting; Figure S3. Schematic of randomised complete block experimental design; Figure S4. Relative percentage of each of the causes of fruit rejection in the unmarketable production for each treatment.

Author Contributions: Conceptualisation and methodology, F.d.M.T. and D.E.M.A.; formal analysis, F.d.M.T. and R.H.M.; investigation, F.d.M.T., R.H.M. and D.E.M.A.; writing—original draft preparation, F.d.M.T.; writing—review and editing, F.d.M.T., R.H.M. and D.E.M.A. All authors have read and agreed to the published version of the manuscript.

Funding: This research did not receive any specific grant from funding agencies in the public, commercial, or not-for-profit sectors. Nevertheless, we would like to thank the “María Zambrano” grant awarded to Rafael Hernández Maqueda (María Zambrano, UAL, Ministry of Universities, Recovery, Transformation and Resilience Plan funded by the European Union-Next Generation EU).

Data Availability Statement: The data from this research are available upon request via e-mail at fmoral@ual.es.

Acknowledgments: We would like to thank the Fundación Cajamar Finca Experimental “Palmerillas” for their collaboration in supporting the experiments, the company Nanobubbles S.L. for providing the nanobubble generating equipment, and Francisco Manuel Padilla Ruiz for his advice in determining the root distribution.

Conflicts of Interest: The authors declare no conflicts of interest.

References

1. Ben-Noah, I.; Nitsan, I.; Cohen, B.; Kaplan, G.; Friedman, S.P. Soil Aeration Using Air Injection in a Citrus Orchard with Shallow Groundwater. *Agric. Water Manag.* **2021**, *245*, 106664. [[CrossRef](#)]
2. Pineda Pineda, J.; Moreno Roblero, M.d.J.; Colinas León, M.T.; Sahagún Castellanos, J. El Oxígeno En La Zona Radical y Su Efecto En Las Plantas. *Rev. Mex. Cienc. Agric.* **2020**, *11*, 931–943. [[CrossRef](#)]
3. Carazo, N. Oxifertirrigación En Cultivo Sin Suelo de Rosa Para Flor Cortada (Rosa Sp.) y Pimiento (*Capsicum annuum* L.): Efectos En Desarrollo y Producción. Ph.D. Thesis, Universidad de Lleida, Lleida, Spain, 2015.
4. Bhattacharai, S.P.; Su, N.; Midmore, D.J. Oxygation Unlocks Yield Potentials of Crops in Oxygen-Limited Soil Environments. *Adv. Agron.* **2005**, *88*, 313–377. [[CrossRef](#)]
5. Jin, C.; Lei, H.; Chen, J.; Xiao, Z.; Leghari, S.J.; Yuan, T.; Pan, H. Effect of Soil Aeration and Root Morphology on Yield under Aerated Irrigation. *Agronomy* **2023**, *13*, 369. [[CrossRef](#)]
6. Dresbøll, D.B.; Thorup-Kristensen, K. Spatial Variation in Root System Activity of Tomato (*Solanum lycopersicum* L.) in Response to Short and Long-Term Waterlogging as Determined by ^{15}N Uptake. *Plant Soil.* **2012**, *357*, 161–172. [[CrossRef](#)]
7. Ben-Noah, I.; Friedman, S.P. Review and Evaluation of Root Respiration and of Natural and Agricultural Processes of Soil Aeration. *Vadose Zone J.* **2018**, *17*, 1–47. [[CrossRef](#)]
8. Abuarab, M.; Mostafa, E.; Ibrahim, M. Effect of Air Injection under Subsurface Drip Irrigation on Yield and Water Use Efficiency of Corn in a Sandy Clay Loam Soil. *J. Adv. Res.* **2013**, *4*, 493–499. [[CrossRef](#)] [[PubMed](#)]
9. Bhattacharai, S.P.; Pendergast, L.; Midmore, D.J. Root Aeration Improves Yield and Water Use Efficiency of Tomato in Heavy Clay and Saline Soils. *Sci. Hortic.* **2006**, *108*, 278–288. [[CrossRef](#)]
10. Vyrlas, P.; Sakellarou-Makrantonaki, M.; Kalfoountzos, D. Aerogation: Crop Root-Zone Aeration through Subsurface Drip Irrigation System. *WSEAS Trans. Environ. Dev.* **2014**, *10*, 250–255.
11. Pendergast, L.; Bhattacharai, S.P.; Midmore, D.J. Evaluation of Aerated Subsurface Drip Irrigation on Yield, Dry Weight Partitioning and Water Use Efficiency of a Broad-Acre Chickpea (*Cicer arietinum*, L.) in a Vertisol. *Agric. Water Manag.* **2019**, *217*, 38–46. [[CrossRef](#)]
12. Zhao, F.; Sun, J.; Jiang, Y.; Hu, D.; Yang, X.; Dong, M.; Yu, K.; Yu, S. Effect of Rhizosphere Aeration by Subsurface Drip Irrigation with Tanks on the Growth of ‘Red Globe’ Grape Seedling and Its Absorption, Distribution and Utilization of Urea- ^{15}N . *Sci. Hortic.* **2018**, *236*, 207–213. [[CrossRef](#)]

13. Park, J.S.; Ohashi, K.; Kurata, K.; Lee, J.W. Promotion of Lettuce Growth by Application of Microbubbles in Nutrient Solution Using Different Rates of Electrical Conductivity and under Periodic Intermittent Generation in a Deep Flow Technique Culture System. *Eur. J. Hortic. Sci.* **2010**, *75*, 198–203.
14. Abu-Shahba, M.S.; Mansour, M.M.; Mohamed, H.I.; Sofy, M.R. Comparative Cultivation and Biochemical Analysis of Iceberg Lettuce Grown in Sand Soil and Hydroponics With or Without Microbubbles and Macrobubbles. *J. Soil. Sci. Plant Nutr.* **2021**, *21*, 389–403. [CrossRef]
15. Quan, L.-J.; Zhang, B.; Shi, W.-W.; Li, H.-Y. Hydrogen Peroxide in Plants: A Versatile Molecule of the Reactive Oxygen Species Network. *J. Integr. Plant Biol.* **2008**, *50*, 2–18. [CrossRef] [PubMed]
16. Abd Elhady, S.A.; El-Gawad, H.G.A.; Ibrahim, M.F.M.; Mukherjee, S.; Elkelish, A.; Azab, E.; Gobouri, A.A.; Farag, R.; Ibrahim, H.A.; El-Azm, N.A. Hydrogen Peroxide Supplementation in Irrigation Water Alleviates Drought Stress and Boosts Growth and Productivity of Potato Plants. *Sustainability* **2021**, *13*, 899. [CrossRef]
17. Urrestarazu, M.; Mazuela, P.C. Effect of Slow-Release Oxygen Supply by Fertigation on Horticultural Crops under Soilless Culture. *Sci. Hortic.* **2005**, *106*, 484–490. [CrossRef]
18. Hou, J.; Zhang, D.; Zhou, J.; Xu, Z.; Mou, P.; Cao, Y.; Zhu, J. Oxygenated Compound Fertilizer Improved Rice Yield by Empowering Soil Aeration. *Commun. Soil. Sci. Plant Anal.* **2021**, *52*, 1798–1810. [CrossRef]
19. Wang, R.; Shi, W.; Kronzucker, H.J.; Li, Y. Oxygenation Promotes Vegetable Growth by Enhancing P Nutrient Availability and Facilitating a Stable Soil Bacterial Community in Compacted Soil. *Soil. Tillage Res.* **2023**, *230*, 105686. [CrossRef]
20. Wang, R.; Shi, W.; Li, Y. Link Between Aeration in the Rhizosphere and P-Acquisition Strategies: Constructing Efficient Vegetable Root Morphology. *Front. Environ. Sci.* **2022**, *10*, 906893. [CrossRef]
21. Carrasco, G.; Gajardo, J.M.; Álvaro, J.E.; Urrestarazu, M. Rocket Production (*Eruca sativa* Mill.) in a Floating System Using Peracetic Acid as Oxygen Source Compared with Substrate Culture. *J. Plant Nutr.* **2011**, *34*, 1397–1401. [CrossRef]
22. Du, Y.D.; Niu, W.Q.; Gu, X.B.; Zhang, Q.; Cui, B.J.; Zhao, Y. Crop Yield and Water Use Efficiency under Aerated Irrigation: A Meta-Analysis. *Agric. Water Manag.* **2018**, *210*, 158–164. [CrossRef]
23. Li, Y.; Jia, Z.; Niu, W.; Wang, J.; Zhang, M. Effect of Post-Infiltration Soil Aeration at Different Growth Stages on Growth and Fruit Quality of Drip-Irrigated Potted Tomato Plants (*Solanum lycopersicum*). *PLoS ONE* **2015**, *10*, e0143322. [CrossRef] [PubMed]
24. Bonachela, S.; Quesada, J.; Acuña, R.A.; Magán, J.J.; Marfà, O. Oxyfertigation of a Greenhouse Tomato Crop Grown on Rockwool Slabs and Irrigated with Treated Wastewater: Oxygen Content Dynamics and Crop Response. *Agric. Water Manag.* **2010**, *97*, 433–438. [CrossRef]
25. Baram, S.; Weinstein, M.; Evans, J.F.; Berezkin, A.; Sade, Y.; Ben-Hur, M.; Bernstein, N.; Mamane, H. Drip Irrigation with Nanobubble Oxygenated Treated Wastewater Improves Soil Aeration. *Sci. Hortic.* **2022**, *291*, 110550. [CrossRef]
26. Ben-Noah, I.; Friedman, S.P. Aeration of Clayey Soils by Injecting Air through Subsurface Drippers: Lysimetric and Field Experiments. *Agric. Water Manag.* **2016**, *176*, 222–233. [CrossRef]
27. Friedman, S.P.; Naftaliev, B. A Survey of the Aeration Status of Drip-Irrigated Orchards. *Agric. Water Manag.* **2012**, *115*, 132–147. [CrossRef]
28. Bhattarai, S.P.; Huber, S.; Midmore, D.J. Aerated Subsurface Irrigation Water Gives Growth and Yield Benefits to Zucchini, Vegetable Soybean and Cotton in Heavy Clay Soils. *Ann. Appl. Biol.* **2004**, *144*, 285–298. [CrossRef]
29. Bhattarai, S.P.; Midmore, D.J.; Pendergast, L. Yield, Water-Use Efficiencies and Root Distribution of Soybean, Chickpea and Pumpkin under Different Subsurface Drip Irrigation Depths and Oxygation Treatments in Vertisols. *Irrig. Sci.* **2008**, *26*, 439–450. [CrossRef]
30. Zhu, Y.; Cai, H.; Song, L.; Chen, H. Aerated Irrigation Promotes Soil Respiration and Microorganism Abundance around Tomato Rhizosphere. *Soil. Sci. Soc. Am. J.* **2019**, *83*, 1343–1355. [CrossRef]
31. Agarwal, A.; Ng, W.J.; Liu, Y. Principle and Applications of Microbubble and Nanobubble Technology for Water Treatment. *Chemosphere* **2011**, *84*, 1175–1180. [CrossRef]
32. Foudas, A.W.; Kosheleva, R.I.; Favvas, E.P.; Kostoglou, M.; Mitropoulos, A.C.; Kyza, G.Z. Fundamentals and Applications of Nanobubbles: A Review. *Chem. Eng. Res. Des.* **2023**, *189*, 64–86. [CrossRef]
33. Ghaani, M.R.; Kusalik, P.G.; English, N.J. Massive Generation of Metastable Bulk Nanobubbles in Water by External Electric Fields. *Sci. Adv.* **2020**, *6*, eaaz0094. [CrossRef]
34. Zhang, Z.-H.; Wang, S.; Cheng, L.; Ma, H.; Gao, X.; Brennan, C.S.; Yan, J.-K. Micro-Nano-Bubble Technology and Its Applications in Food Industry: A Critical Review. *Food Rev. Int.* **2022**, *39*, 4213–4235. [CrossRef]
35. Azevedo, A.; Oliveira, H.; Rubio, J. Bulk Nanobubbles in the Mineral and Environmental Areas: Updating Research and Applications. *Adv. Colloid. Interface Sci.* **2019**, *271*, 101992. [CrossRef] [PubMed]
36. Marcelino, K.R.; Ling, L.; Wongkiew, S.; Nhan, H.T.; Surendra, K.C.; Shitanaka, T.; Lu, H.; Khanal, S.K. Nanobubble Technology Applications in Environmental and Agricultural Systems: Opportunities and Challenges. *Crit. Rev. Environ. Sci. Technol.* **2022**, *53*, 1378–1403. [CrossRef]
37. Salinas, J.; Meca, D.; del Moral, F. Short-Term Effects of Changing Soil Management Practices on Soil Quality Indicators and Crop Yields in Greenhouses. *Agronomy* **2020**, *10*, 582. [CrossRef]
38. Fernández, M.D.; Baeza, E.; Céspedes, A.; Pérez-Parra, J.; Gázquez, J.C. Validation Of On-Farm Crop Water Requirements (Prho) Model for Horticultural Crops in an Unheated Plastic Greenhouse. *Acta Hortic.* **2009**, *807*, 295–300. [CrossRef]

39. Padilla, F.M.; Peña-Fleitas, M.T.; Fernández, M.D.; del Moral, F.; Thompson, R.B.; Gallardo, M. Responses of Soil Properties, Crop Yield and Root Growth to Improved Irrigation and N Fertilization, Soil Tillage and Compost Addition in a Pepper Crop. *Sci. Hortic.* **2017**, *225*, 422–430. [[CrossRef](#)]
40. Eklund, F.; Alheshibri, M.; Swenson, J. Differentiating Bulk Nanobubbles from Nanodroplets and Nanoparticles. *Curr. Opin. Colloid. Interface Sci.* **2021**, *53*, 101427. [[CrossRef](#)]
41. Cerrón-Calle, G.A.; Luna Magdaleno, A.; Graf, J.C.; Apul, O.G.; García-Segura, S. Elucidating CO₂ Nanobubble Interfacial Reactivity and Impacts on Water Chemistry. *J. Colloid. Interface Sci.* **2021**, *607*, 720–728. [[CrossRef](#)]
42. Mingorance, M.D.D.; Barahona, E.; Fernández-Gálvez, J. Guidelines for Improving Organic Carbon Recovery by the Wet Oxidation Method. *Chemosphere* **2007**, *68*, 409–413. [[CrossRef](#)] [[PubMed](#)]
43. Mulvaney, R.L. *Methods of Soil Analysis*; Sparks, D.L., Page, A.L., Helmke, P.A., Loepert, R.H., Soltanpour, P.N., Tabatabai, M.A., Johnston, C.T., Sumner, M.E., Eds.; SSSA Book Series; Soil Science Society of America, American Society of Agronomy: Madison, WI, USA, 1996; ISBN 9780891188667.
44. FAO. *Standard Operating Procedure for Soil Available Phosphorus*; FAO, Ed.; FAO: Rome, Italy, 2021.
45. Peña-Fleitas, M.T.; Gallardo, M.; Thompson, R.B.; Farneselli, M.; Padilla, F.M. Assessing Crop N Status of Fertigated Vegetable Crops Using Plant and Soil Monitoring Techniques. *Ann. Appl. Biol.* **2015**, *167*, 387–405. [[CrossRef](#)] [[PubMed](#)]
46. Hochmuth, G.; Hochmuth, R. Plant Petiole Sap-Testing for Vegetable Crops. *EDIS* **2022**, *2022*, 1–6. [[CrossRef](#)]
47. Vignoni, L.A.; Césari, R.M.; Forte, M.; Mirábole, M.L. Determinación de Indice de Color En Ajo Picado. *Inf. Tecnológica* **2006**, *17*, 63–67. [[CrossRef](#)]
48. Benito-Bautista, P.; Arellanes-Juárez, N.; Pérez-Flores, M.E. Color y Estado de Madurez Del Fruto de Tomate de Cáscara. *Agron. Mesoam.* **2015**, *27*, 115. [[CrossRef](#)]
49. Ashebir, D.; Jezik, K.; Weingartemann, H.; Gretzmacher, R. Change in Color and Other Fruit Quality Characteristics of Tomato Cultivars after Hot-Air Drying at Low Final-Moisture Content. *Int. J. Food Sci. Nutr.* **2009**, *60*, 308–315. [[CrossRef](#)]
50. Barreiro, J.A.; Milano, M.; Sandoval, A.J. Kinetics of Colour Change of Double Concentrated Tomato Paste during Thermal Treatment. *J. Food Eng.* **1997**, *33*, 359–371. [[CrossRef](#)]
51. Soare, R.; Dinu, M.; Apahidean, A.-I.; Soare, M. The Evolution of Some Nutritional Parameters of the Tomato Fruit during the Harvesting Stages. *Hortic. Sci.* **2019**, *46*, 132–137. [[CrossRef](#)]
52. Javanmardi, J.; Kubota, C. Variation of Lycopene, Antioxidant Activity, Total Soluble Solids and Weight Loss of Tomato during Postharvest Storage. *Postharvest Biol. Technol.* **2006**, *41*, 151–155. [[CrossRef](#)]
53. Donald, C.M.; Hamblin, J. The Biological Yield and Harvest Index of Cereals as Agronomic and Plant Breeding Criteria. *Adv. Agron.* **1976**, *28*, 361–405.
54. Sukor, A.; Qian, Y.; Davis, J.G. Organic Nitrogen Fertilizer Selection Influences Water Use Efficiency in Drip-Irrigated Sweet Corn. *Agriculture* **2023**, *13*, 923. [[CrossRef](#)]
55. Fageria, N.K.; Baligar, V.C. Enhancing Nitrogen Use Efficiency in Crop Plants. *Adv. Agron.* **2005**, *88*, 97–185. [[CrossRef](#)]
56. Baram, S.; Evans, J.F.; Berezkin, A.; Ben-Hur, M. Irrigation with Treated Wastewater Containing Nanobubbles to Aerate Soils and Reduce Nitrous Oxide Emissions. *J. Clean. Prod.* **2021**, *280*, 124509. [[CrossRef](#)]
57. Liu, Y.; Zhou, Y.; Wang, T.; Pan, J.; Zhou, B.; Muhammad, T.; Zhou, C.; Li, Y. Micro-Nano Bubble Water Oxygation: Synergistically Improving Irrigation Water Use Efficiency, Crop Yield and Quality. *J. Clean. Prod.* **2019**, *222*, 835–843. [[CrossRef](#)]
58. Wu, Y.; Lyu, T.; Yue, B.; Tonoli, E.; Verderio, E.A.M.; Ma, Y.; Pan, G. Enhancement of Tomato Plant Growth and Productivity in Organic Farming by Agri-Nanotechnology Using Nanobubble Oxygation. *J. Agric. Food Chem.* **2019**, *67*, 10823–10831. [[CrossRef](#)] [[PubMed](#)]
59. Chen, W.; Bastida, F.; Liu, Y.; Zhou, Y.; He, J.; Song, P.; Kuang, N.; Li, Y. Nanobubble Oxygenated Increases Crop Production via Soil Structure Improvement: The Perspective of Microbially Mediated Effects. *Agric. Water Manag.* **2023**, *282*, 108263. [[CrossRef](#)]
60. Zhu, Y.; Dyck, M.; Cai, H.J.; Song, L.B.; Chen, H. The Effects of Aerated Irrigation on Soil Respiration, Oxygen, and Porosity. *J. Integr. Agric.* **2019**, *18*, 2854–2868. [[CrossRef](#)]
61. Bonachela, S.; Fernández, M.D.; Cabrera, F.J.; Granados, M.R. Soil Spatio-Temporal Distribution of Water, Salts and Nutrients in Greenhouse, Drip-Irrigated Tomato Crops Using Lysimetry and Dielectric Methods. *Agric. Water Manag.* **2018**, *203*, 151–161. [[CrossRef](#)]
62. Bonachela, S.; Acuña, R.A.; Casas, J. Environmental Factors and Management Practices Controlling Oxygen Dynamics in Agricultural Irrigation Ponds in a Semiarid Mediterranean Region: Implications for Pond Agricultural Functions. *Water Res.* **2007**, *41*, 1225–1234. [[CrossRef](#)]
63. Grasso, R.; Peña-Fleitas, M.T.; Gallardo, M.; Thompson, R.B.; Padilla, F.M. Tillage Effects on Soil Properties, Crop Responses and Root Density of Sweet Pepper (*Capsicum Annuum*). *Span. J. Agric. Res.* **2021**, *19*, e0902. [[CrossRef](#)]
64. Niu, W.; Jia, Z.; Zhang, X.; Shao, H. Effects of Soil Rhizosphere Aeration on the Root Growth and Water Absorption of Tomato. *Clean (Weinh)* **2012**, *40*, 1364–1371. [[CrossRef](#)]
65. Rasmussen, I.S.; Dresbøll, D.B.; Thorup-Kristensen, K. Winter Wheat Cultivars and Nitrogen (N) Fertilization—Effects on Root Growth, N Uptake Efficiency and N Use Efficiency. *Eur. J. Agron.* **2015**, *68*, 38–49. [[CrossRef](#)]
66. Birlanga, V.; Acosta-Motos, J.R.; Pérez-Pérez, J.M. Mitigation of Calcium-Related Disorders in Soilless Production Systems. *Agronomy* **2022**, *12*, 644. [[CrossRef](#)]

67. Wang, J.; Cui, Y.; Wu, K.; Wu, S.; Wu, K.; Li, Y.; Niu, W. Micro/Nanobubble-Aerated Drip Irrigation Affects Saline Soil Microenvironments and Tomato Growth by Altering Bacterial Communities. *Soil Tillage Res.* **2024**, *239*, 106034. [[CrossRef](#)]
68. Zhou, Y.; Bastida, F.; Liu, Y.; He, J.; Chen, W.; Wang, X.; Xiao, Y.; Song, P.; Li, Y. Impacts and Mechanisms of Nanobubbles Level in Drip Irrigation System on Soil Fertility, Water Use Efficiency and Crop Production: The Perspective of Soil Microbial Community. *J. Clean. Prod.* **2021**, *333*, 130050. [[CrossRef](#)]
69. Osorio, S.; Ruan, Y.L.; Fernie, A.R. An Update on Source-to-Sink Carbon Partitioning in Tomato. *Front. Plant Sci.* **2014**, *5*, 516. [[CrossRef](#)]
70. Bénard, C.; Gautier, H.; Bourgaud, F.; Grasselly, D.; Navez, B.; Caris-Veyrat, C.; Weiss, M.; Génard, M. Effects of Low Nitrogen Supply on Tomato (*Solanum lycopersicum*) Fruit Yield and Quality with Special Emphasis on Sugars, Acids, Ascorbate, Carotenoids, and Phenolic Compounds. *J. Agric. Food Chem.* **2009**, *57*, 4112–4123. [[CrossRef](#)] [[PubMed](#)]
71. Pavan, M.P.; Gangaprasad, S.; Adivappar, N. Genetic Variability, Trait Inter-Relationships, Third and Fourth Degree Statistics Based Genetics for Fruit Quality and Yield Traits Governing Shelf Life in Tomato (*Solanum lycopersicum* L.). *Plant Genet. Resour.* **2022**, *20*, 366–375. [[CrossRef](#)]
72. Cvikić, D.; Zdravković, J.; Pavlović, N.; Adžić, S.; Dordević, M. Postharvest Shelf Life of Tomato (*Lycopersicon esculentum* Mill.) Mutanats (nor and Rin) and Their Hybrids. *Genetika* **2012**, *44*, 449–456. [[CrossRef](#)]
73. Felföldi, Z.; Ranga, F.; Roman, I.A.; Sestras, A.F.; Vodnar, D.C.; Prohens, J.; Sestras, R.E. Analysis of Physico-Chemical and Organoleptic Fruit Parameters Relevant for Tomato Quality. *Agronomy* **2022**, *12*, 1232. [[CrossRef](#)]
74. Zhu, Y.; Cai, H.J.; Song, L.B.; Shang, Z.H.; Chen, H. Comprehensive Evaluation of Different Oxygation Treatments Based on Fruit Yield and Quality of Greenhouse Tomato. *Sci. Agric. Sin.* **2020**, *53*, 2241–2252.
75. Zhou, Y.; Zhou, B.; Xu, F.; Muhammad, T.; Li, Y. Appropriate Dissolved Oxygen Concentration and Application Stage of Micro-Nano Bubble Water Oxygation in Greenhouse Crop Plantation. *Agric. Water Manag.* **2019**, *223*, 105713. [[CrossRef](#)]
76. Dumas, Y.; Dadomo, M.; Di Lucca, G.; Grolier, P. Effects of Environmental Factors and Agricultural Techniques on Antioxidant Content of Tomatoes. *J. Sci. Food Agric.* **2003**, *83*, 369–382. [[CrossRef](#)]
77. Yao, Y.; Zhao, Z.; Ding, Z.; Yao, K.; Yang, Y.; Hou, X.; Li, C.; Zhang, H.; Li, Y.; Wang, C.; et al. Hydrogen-Rich Water Irrigation Promotes Fruit Ripening and Nutritional Composition in Tomato. *Postharvest Biol. Technol.* **2024**, *213*, 112920. [[CrossRef](#)]

Disclaimer/Publisher's Note: The statements, opinions and data contained in all publications are solely those of the individual author(s) and contributor(s) and not of MDPI and/or the editor(s). MDPI and/or the editor(s) disclaim responsibility for any injury to people or property resulting from any ideas, methods, instructions or products referred to in the content.